Published in final edited form as:
Synapse. 2011 August ; 65(8): 804–813. doi:10.1002/syn.20907.

Mefloquine Effects on Ventral Tegmental Area Dopamine and GABA Neuron Inhibition: A Physiologic Role for Connexin-36 Gap Junctions

DAVID W. ALLISON, **REBECCA S. WILCOX**, **KYLE L. ELLEFSEN**, **CAITLIN E. ASKEW**, **DAVID M. HANSEN**, **JEFFREY D. WILCOX**, **STEPHANIE S. SANDOVAL**, **DENNIS L. EGGETT**, **YUCHIO YANAGAWA**, and **SCOTT C. STEFFENSEN**[*]
Brigham Young University, Provo, Utah 84602

Abstract

Connexin-36 (Cx36) gap junctions (GJs) appear to be involved in the synchronization of GABA interneurons in many brain areas. We have previously identified a population of Cx36-connected ventral tegmental area (VTA) GABA neurons that may regulate mesolimbic dopamine (DA) neurotransmission, a system implicated in reward from both natural behaviors and drugs of abuse. The aim of this study was to determine the effect mefloquine (MFQ) has on midbrain DA and GABA neuron inhibition, and the role Cx36 GJs play in regulating midbrain VTA DA neuron activity in mice. In brain slices from adolescent wild-type (WT) mice the Cx36-selective GJ blocker mefloquine (MFQ, 25 μM) increased VTA DA neuron sIPSC frequency sixfold, and mIPSC frequency threefold. However, in Cx36 KO mice, MFQ only increased sIPSC and mIPSC frequency threefold. The nonselective GJ blocker carbenoxolone (CBX, 100 μM) increased DA neuron sIPSC frequency twofold in WT mice, did not affect Cx36 KO mouse sIPSCs, and did not affect mIPSCs in WT or Cx36 KO mice. Interestingly, MFQ had no effect on VTA GABA neuron sIPSC frequency. We also examined MFQ effects on VTA DA neuron firing rate and current-evoked spiking in WT and Cx36 KO mice, and found that MFQ decreased WT DA neuron firing rate and current-evoked spiking, but did not alter these measures in Cx36 KO mice. Taken together these findings suggest that blocking Cx36 GJs increases VTA DA neuron inhibition, and that GJs play in key role in regulating inhibition of VTA DA neurons.

Keywords

IPSC; Cx36; VTA; interneuron; carbenoxolone; mouse; midbrain; malaria

INTRODUCTION

The mesolimbic dopamine (DA) pathway is composed of DA neurons in the ventral tegmental area (VTA) of the midbrain that project to the dorsal striatum, hippocampus, amygdala, and prefrontal cortex (for review see Wise, 2004). This diffuse modulatory

[*]Correspondence to: Scott C. Steffensen, Department of Psychology Center for Neuroscience (1050 SWKT); Brigham Young University; Utah 84602. scott_steffensen@byu.edu.

pathway is involved in attention to rewarding stimuli, learned behavior, and drug addiction (for reviews Fields et al., 2007; Ikemoto, 2007). It is believed that VTA DA neurons are inhibited by local GABA interneurons, and projection GABA neurons from other brain regions (Johnson and North, 1992; Steffensen et al., 1998). There is evidence suggesting that this DA pathway contains reciprocal excitatory and GABAergic communication with other brain regions (Carr and Sesack, 2000a,b; Margolis et al., 2008; Omelchenko and Sesack, 2005, 2006). Ventral tegmental area GABA neurons express Connexin-36 (Cx36) gap junctions (GJs; (Allison et al., 2006)), dye couple (Allison et al., 2006; Steffensen et al., 1998), and form part of a larger syncytium of GABA neurons in the reticular formation that are linked by Cx36 electrical synapses (Lassen et al., 2007). Acute intoxicating doses of ethanol and GJ antagonists, including the Cx36-selective antagonist mefloquine (MFQ), suppress electrical coupling between VTA GABA neurons in vivo (Allison et al., 2006; Stobbs et al., 2004).

While the role of GJs in the adult brain is not known, they are thought to play a role in the intercellular spread of ions, small molecules, and the propagation of oscillatory patterns (Landisman and Connors, 2005) and spike synchrony (Galarreta and Hestrin, 2001; Szabadics et al., 2001). Studying Cx36 GJ's is made difficult by the lack of drugs that act specifically and exclusively on GJs, and most promising are MFQ, a Cx36-selective GJ blocker, and carbenoxolone (CBX), both of which have non-GJ blocking affects (for review Juszczak and Swiergiel, 2009). Despite the shortcomings of these drugs, they can be utilized to determine the neurophysiology of GJs in appropriately designed and executed experiments that control for nonspecific effects. Mefloquine is a potent antimalarial prophylaxis and treatment, but owing to its ability to cross the blood-brain barrier and accumulate to high concentrations, it has been linked to adverse side-effects ranging in severity from mild dysphoria to severe psychotic episodes or seizures (Schlagenhauf et al., 2009; Tran et al., 2006; Wooltorton, 2002). While MFQ's neuropsychiatric side-effects have not been attributed to a specific pharmacological action, they may derive from its ability to affect synaptic activity. Owing to DA's involvement in synaptic transmission, mood, reward and addiction, we hypothesized that some of MFQ's side-effects may result from MFQ's blockade of Cx36 GJs in the VTA, and point to the possible role for Cx36 GJs in regulation of DA. We hypothesized that MFQ's blockade Cx36 GJs might disrupt the network activity of electrically coupled VTA GABA neurons, thereby altering inhibition of VTA DA neurons resulting in a change in DA neuron activity. We investigated the effects of MFQ and CBX on DA and GABA neuron inhibitory synaptic activity in wild-type (WT) and Cx36 knock-out (KO) mice.

METHODS

Animal subjects

The care and use of animals and experimental protocols were approved by the Institutional Animal Care and Use Committee (IACUC) of Brigham Young University. This study was conducted in 21 to 35 D.O. juvenile male mice. Two different mouse models were used in this study; a glutamate decarboxylase-67 (GAD67)-green fluorescent protein (GFP) knock-in mouse (Tamamaki et al., 2003), and a Cx36 knock-out (KO) mouse (Deans et al., 2001).

The GAD67-GFP knock-in mice were created on a CD-1 background strain and afforded us the ability in some experiments to positively identify and record from GAD67-positive GABA neurons in the VTA via fluorescence microscopy. The Cx36 KO mice were created on a C57BL6 background, which were used as wild-type (WT) controls. The Cx36 coding sequence was replaced by a LacZ-IRES-PLAP reporter cassette (Deans et al., 2001). Activation of the Cx36 promoter results in expression of the cytoplasmic protein β-gal. Neurons that would normally generate Cx36 transcripts expressed the β-gal reporter throughout their cytoplasmic domain. The Cx36 KO mice provided a comparison against MFQ's Cx36 GJ blocking effects on VTA DA neurons in GAD67-GFP knock-in mice.

Preparation of brain slices

Midbrain slices were obtained as previously described (Steffensen et al., 2008). Briefly, mice were anesthetized with Ketamine (60 mg/kg), decapitated, and brains were quickly dissected and sectioned into 200 μm thick horizontal slices in ice-cold artificial cerebrospinal fluid (ACSF), bubbled with 95% O2/5% CO2. This cutting solution consisted of (in mM): 220 Sucrose, 3 KCl, 1.25 NaH2PO4, 25 NaH2CO3, 12 MgSO4, 10 Glucose, 0.2 CaCl2, and 0.4 Ketamine. These VTA-targeted horizontal slices were immediately placed into an incubation chamber containing normal ACSF bubbled with 95% O_2/5% CO_2 at 34–35° consisting of (in mM): 124 NaCl, 3 KCl, 1.25 NaH_2PO_4, 26 $NaHCO_3$, 12 glucose, 1.5 $MgSO_4$, 2 $CaCl_2$, pH 7.3, and allowed to incubate for at least 45 min prior to being transferred to a recording chamber. Once transferred to a recording chamber with continuous normal ACSF flow (2.0 ml/min) the temperature was maintained at 34–35° throughout the experiment. Brain slices where also allowed to settle in the recording chamber for an additional 15 min before recordings began. Cells were visualized with either a Nikon Eclipse FN1 or E600FN microscope in the transmitted de Sénarmont Differential Interference Contrast (DIC)/infrared (IR) configuration.

Whole-cell recordings in vitro

Electrodes pulled from borosilicate glass capillary tubes were filled with one of two types of pipette solutions consisting of either (in mM): 128 KCl, 20 NaCl, 0.3 $CaCl_2$, 1.2 $MgCl_2$, 10 HEPES, 1 EGTA, 2 Mg-ATP, 0.25 Na-GTP (pH 7.3) for IPSCs, and 123 K-Gluconate, 8 NaCl, 10 HEPES, 0.2 EGTA, 2 Mg-ATP, 2 Na3-GTP (pH 7.3) for firing rate experiments. Pipettes had tip resistances of 2.5–4 MΩ, and series resistances typically ranging from 7 to 15 MΩ. Access resistance (R_a, typically 100 to 300 MΩ) and membrane resistance (R_m), were continuously monitored with a 5 mV voltage step delivered every 10 s throughout experiments. Only experiments that maintained stable R_a and R_m (less than 15% change) were included in this study. Voltage clamp recordings were filtered at 2 kHz while current-drive spikes were filtered at 10 kHz with an Axon Instruments Multiclamp 700B amplifier and digitized at 5 to 20 kHz respectively using an Axon 1440A digitizer. Axon Instruments pClamp ver10, Mini Analysis (Synapt-soft: Decatur, GA), and Igor Pro (Wavemetrics: Oswego, OR) software packages were utilized for data collection and analysis. Evoked and spontaneous IPSCs (sIPSCs) were recorded in the presence of D-2-amino-5-phosphonopentanoic acid (D-APV, 50 μM), 6-cyano-23-dihydroxy-7-nitro-quinoxaline (CNQX, 30 μM), and eticlopride (100 nM) to block NMDA, AMPA, and DA D2-mediated synaptic currents respectively. Miniature IPSCs (mIPSCs) were isolated from all other

spontaneous activity by addition of lidocaine (500 μM), as TTX does not block all types of voltagegated sodium channels (Melis et al., 2002; Steffensen et al., 2008). All sIPSCs were inward at the holding potential of –70 mV and were completely blocked by bicuculline.

For determination of spontaneous synaptic current rate, the amplitude threshold was set to 5X root-mean-square amplitude, and area threshold was maximized for inhibitory currents. Spontaneous and mini currents were automatically detected, verified, and corrected by visual inspection of the recordings. Firing rate was calculated by comparing 5 min of control and test data.

Drug preparation and administration

Mefloquine was prepared fresh at a concentration of 1 mg/ml in water to obtain a 25 mM stock solution. In experiments where brain slices were allowed to pre-soak in normal ACSF 1 drug(s), drugs were added to the slice incubation chamber and allowed to presoak 45 to 60 min, then continuously perfused throughout the experiment. There are two advantages to presoaking slices with drugs such as MFQ and CBX compared to obtaining a viable recording and then superfusing MFQ and CBX acutely. First, any postsynaptic MFQ effects due to disruption of neuronal calcium levels that develop over time are not washed out by pipette solution. Second, given that long quality recording periods can be problematical using the whole-cell patch-clamp technique, presoaking enables long drug application times which allow for drugs such as MFQ to take full effect and more closely mimic the chronic exposure to MFQ in humans. Indeed, most of MFQ's effects resolved at 1 h after administration, a time course that is problematical for patch clamp recordings using acute superfusion.

Characterization of neuron types

Neurons in the VTA of GAD67-GFP WT and Cx36 KO mice that exhibited a modest noncation specific inward rectifying current (I_h) in combination with low input resistance were assumed to be DA neurons (Allison et al., 2006; Johnson and North, 1992; Margolis et al., 2006). In GAD67 GFP knock-in mice, GABA neurons were identified with the aid of fluorescence microscopy. Only neurons located in the VTA that exhibited robust GFP fluorescence were considered GABAergic (Tamamaki et al., 2003).

Statistical analyses

All results are presented as raw mean values and percent control ±SEM. Results between groups were compared using a two-tailed unpaired *t*-test or ANOVA. Experiments relying on variance in time or current were analyzed using mixed models ANOVA with post hoc *t*-test at individual points. Statistical significance required ≥95% level of confidence ($P \leq 0.05$). Analysis software included Statistical Analysis Software (SAS Institute, Inc), Microsoft Excel, and Igor Pro (Wavemetrics, Oswego, OR). Significance levels are indicated on graphs with asterisks *,**,*** and correspond to significance levels $P < 0.05$, 0.01 and 0.001, respectively. Figures were constructed with Igor Pro software.

RESULTS

Time course of mefloquine effects on *VTA Dopamine Neuron* sIPSC frequency

Others have shown that the Connexin-36 (Cx36) gap junction (GJ) blocker mefloquine (MFQ) increases sIPSCs in substantia nigra pars compacta (SNc) DA neurons ($EC_{50} \approx 3$ μM; (Zhou et al., 2006)). However, the application time of MFQ in that study correlated with MFQ's ability to disrupt intracellular calcium (Dow et al., 2003), rather than its ability to selectively block Cx36 GJs (Cruikshank et al., 2004). We first determined the time required for 25 μM MFQ to reach maximum effect on VTA DA neuron sIPSC frequency, and whether there was a significant difference between WT and Cx36 KO mice in the time course of MFQ's effects. In Figure 1, 25 μM MFQ was bath-applied in the presence of D-APV (50 μM) and CNQX (30 μM) and the frequency of VTA DA neuron sIPSCs was measured at 15-min intervals. The baseline frequency of WT and Cx36 KO sIPSCs at time zero did not differ (7.3 ± 1.7 Hz WT, 7.3 ± 1.0 Hz Cx36 KO, $P > 0.5$). This lack of difference at baseline may be the result of adaptive compensatory mechanisms in KO mice, however, later experiments comparing baseline firing rates between mouse types without GLU receptor blockers showed KO mice have a lower baseline firing rate than WT mice. MFQ significantly increased sIPSC frequency in both WT and KO mice from the 30 min time point onward and reached maximum effect at ≥60 min ($P > 0.0001$, $F = 8.03$, DF = 46 for WT and KO mice) without affecting any change to DA neuron input resistance. However, MFQ's effects on WT and KO mouse sIPSC frequency were significantly different at the ≥60 min time point. WT sIPSC frequency increased to 59.8 ± 4.3 Hz (814.8 ± 7.2% of baseline), while Cx36 KO sIPSC frequency only increased to 32.2 ± 6.5 Hz (441.3 ± 20.4% of baseline, $P = 0.0001$). These sIPSCs were completely eliminated by bicuculline (10 μM, data not shown). Mefloquine's ability to increase sIPSCs in WT and KO mice was not due to changes in cell input resistance, and its ability to increase DA neuron sIPSCs 331% more in WT mice than Cx36 KO mice after 60 min suggested a possible role for GJs in regulating VTA DA neuron inhibition. Gap junctions may serve as resistive loads or current shunts in VTA GABA neurons. If these GJs where dendo-dendritic in nature, their blockade could alter VTA GABA neuron dendrite membrane properties, allowing the cells to depolarize more frequently and lead to increased VTA DA neuron inhibition. Aware that presoaking slices for ≥60 min in MFQ yielded a maximum affect, all remaining recordings in this study were conducted after drugs were presoaked for ≥60 min. All drugs tested, including MFQ, were also included in the perfused ACSF. However, to avoid the possibility that the GLU receptor antagonists CNQX and APV might confound the establishment of MFQ and other drug effects they were only applied to the perfused ACSF in all remaining experiments, and not presoaked with MFQ and other drugs.

Mefloquine effects on *VTA Dopamine* neuron sIPSC frequency, amplitude, and interevent interval

Having established that it takes ≥60 min for MFQ to take full-effect on $GABA_A$ receptor-mediated DA neuron sIPSC frequency in WT and Cx36 KO mice, and that MFQ differentially affects WT and Cx36 mouse DA neuron sIPSCs when applied for ≥60 min, we next compared the effects of presoaked MFQ to other presoaked drugs on VTA DA neuron sIPSC frequency in WT and Cx36 KO mice. Because MFQ has effects other than being a

selective Cx36 GJ blocker, such as increasing intracellular Ca^{21} (Caridha et al., 2008; Dow et al., 2003; Zhou et al., 2006), we compared its effects to carbenoxolone (CBX) in WT and KO mice. We reasoned that if MFQ's GJ blocking properties played a role in increasing sIPSC frequency, a less selective GJ blocker such as CBX, which has no reported effects on intracellular calcium, would increase sIPSC frequency similar to MFQ in WT mice, but not in Cx36 KO mice. In WT mice (Figs. 2A and 2C), presoaking slices in MFQ (25 μM) for ≥60 min markedly increased VTA DA neuron sIPSC frequency from 7.7 ± 0.8 Hz to 40.9 ± 2.7 Hz (533 ± 35.4% of control, $P = 0.0001$, MFQ $n = 28$, control $n = 30$) and CBX (100 μM) moderately increased sIPSC frequency in WT mice from baseline to 16.2 ± 2.2 Hz (210.7 ± 28.3% of control, $P = 0.0001$, CBX $n = 9$, Figs. 2A and 2C). MFQ and CBX shifted the averaged cumulative interevent interval distribution plot to the left (Fig. 2B), suggesting increased activity-dependent, and or nonactivity dependent GABA release.

In Cx36 KO mice, MFQ increased sIPSC frequency from 8.9 ± 1.7 Hz to 27.9 ± 3.7 Hz (311.4 ± 41.1% of control, $P = 0.0003$, control n = 10, MFQ n = 8 Figs. 2D and 2F) which was approximately 58% of its effect in WT mice (Fig. 2C). Opposite to WT mice, CBX did not affect sIPSC frequency in Cx36 KO mice ($P = 0.64$, CBX n = 7, Figs. 2D and 2F) and only MFQ shifted the cumulative sIPSC interevent distribution plot markedly to the left in Cx36 KO mice (Fig. 2E). The difference in MFQ effect on sIPSC frequency between WT and Cx36 KO mice in combination with CBX only increasing sIPSC frequency in WT mice, reinforces the idea that MFQ-induced increases in VTA DA neuron sIPSC frequency in WT mice was due to both its Cx36-specific GJ blocking properties and its ability to disrupt intracellular calcium (Zhou et al., 2006). However MFQ's effects in Cx36 KO mice were only due to its calcium effects.

Recent studies demonstrated MFQ acts as a $5HT_3$ receptor antagonist (Thompson and Lummis, 2008), and Zhou et al. (2006) hypothesized MFQ's increases sIPSC frequency via its calcium-mediated effects by inhibition of cholinesterase (McArdle et al., 2006), thereby increasing GABA release via excess acetylcholine activation of presynaptic nicotinic acetylcholine receptors (nAChRs). To this end, we also examined the effects of the specific $5HT_3$ receptor antagonist odansetron (ODS) on baseline DA neuron sIPSC frequency and the non-α7nAChR antagonist mecamylamine (MEC) on MFQ's increase in sIPSC frequency. Odansetron did not mimic MFQ, but did decrease sIPSC frequency significantly (74 ± 7.1% of control, $P = 0.0006$, ODS $n = 9$, data only shown in bar graph, Fig. 2C). Similarly, MEC did not alter MFQ's increase of DA neuron sIPSC (488 ± 47.3% of control, MFQ + MEC $n = 6$, $P = 0.58$, Fig. 2C), or its shift of the cumulative interevent interval plot to the left (Fig. 2B). Since ODS did not mimic, and MEC did not block MFQ's effects in WT mice, we did not examine these drugs in Cx36 KO mice.

MEfloquine effects on VTA *Dopamine* neuron mIPSC frequency, amplitude, and interevent interval

Spontaneous postsynaptic currents such as sIPSCs are a combination of both spike-dependent (spike-dependent) and nonspike-dependent transmitter release. To determine what portion of MFQ and CBX-induced increase in sIPSC frequency was due to spike and nonspike-dependent GABA release, we examined the effect of MFQ on WT and Cx36 KO

mice VTA DA neuron nonspike-dependent IPSCs or mini IPSC (mIPSC) frequency by adding lidocaine (500 uM) to the ACSF. In both WT and Cx36 mice, presoaking with MFQ (25 μM) increased VTA DA neuron mIPSC frequency significantly. In WT mice, mIPSC frequency was increased from 7.1 ± 1.2 Hz to 21.9 ± 2.7 Hz (289.8 ± 35.5% of control, $P < 0.0001$, control $n = 13$, MFQ $n = 6$, Fig. 3A and 3C) and in Cx36 KO mice from 8.1 ± 1.8 to 29.0 ± 2.15 Hz (358.3 ± 43.0% of control, $P = 0.004$, control $n = 4$, MFQ $n = 5$). A comparison of these findings to MFQ effects on sIPSCs (Fig. 2) demonstrates that perhaps all of the MFQ increase in Cx36 KO mouse VTA DA neuron sIPSCs was due to an increase in mIPSCs, while only half of the MFQ increase in WT sIPSCs was due to an increase in mIPSCs. From this data, and the finding by Zhou et al. (2006) showing a significant portion of the MFQ increase of sIPSCs was due to a nonspecific calcium effect, we theorized that the MFQ increase of mIPSCs in both WT and Cx36 KO mice was due to an increase of intracellular calcium (Caridha et al., 2008; Dow et al., 2003; Zhou et al., 2006), while the increase in sIPSCs in WT mice was due to the blockade of Cx36 GJs. To test this idea, we examined the effects of CBX (100 μM, a GJ blocker with no calcium effects) on WT mouse VTA DA neuron mIPSCs. CBX had no significant effect on WT mIPSC frequency, but significantly reduced mIPSC amplitude from 30.7 ± 6.5 pA to 13.8 ± 0.7 pA (-55.2 ± 2.3%, $P < 0.027$, CBX $n = 11$, Fig. 3A and 3C). Only MFQ shifted the interevent interval plot the left (Fig. 3B). Given that CBX had no effect on Cx36 sIPSC frequency we did not examine its effects on Cx36 KO mIPSCs.

Mefloquine does not affect VTA GABA neuron sIPSC frequency

Mefloquine's increase of VTA DA neuron sIPSC frequency is remarkable. Thus, we examined its effect on VTA GABA neuron sIPSC frequency. Identification of VTA GABA neurons was aided by the use of GAD67-GFP knock-in mice (referred to as WT mice, Tamamaki et al., 2003). Mefloquine (25 μM) increased slightly, but not significantly, sIPSC baseline frequency in VTA GABA neurons from 11.0 ± 1.4 Hz to 13.7 ± 1.9 Hz (124% of control $n = 17$; MFQ $n = 21$, $P = 0.29$, Figs. 4A and 4C). Mefloquine did not significantly alter sIPSC average amplitude or interevent distribution plots compared to control (Figs. 4B and 4C), nor did it alter the interevent interval plot compared with control (Fig. 4C). These findings demonstrate that MFQ's marked increase in VTA DA neuron sIPSC frequency was not a universal phenomenon common to all inhibitory synapses in the VTA.

MFQ reduces VTA *Dopamine Neuron* firing rate and current-evoked spiking

Thus far we determined that MFQ increased VTA DA neuron activity-dependent IPSC frequency through the blockade of Cx36 gap junctions and nonactivity-dependent IPSC activity most-likely through a nonspecific calcium effect, while having no effect on VTA GABA neuron sIPSCs. We next examined whether this increase in $GABA_A$ receptor-mediated sIPSC frequency in VTA DA neurons would yield an alteration in VTA DA neuron resting membrane potential (RMP), spontaneous firing rate, and current-evoked spiking in WT and Cx36 KO mice. We reasoned that if the mechanism of increased sIPSC frequency in VTA DA neurons was the blockade of Cx36 gap junctions, MFQ would reduce WT VTA DA neuron firing rate, and there would be little difference between MFQ-treated WT and Cx36 KO baseline firing rate and current-evoked spiking. As anticipated, MFQ significantly reduced DA neuron firing rate in WT mice from 1.7 ± 0.4 Hz to 0.6 ± 0.3 Hz

(32.8 ± 17.0% of control, control $n = 11$, MFQ = 9, $P = 0.036$, Figs. 5A and 5B) and significantly reduced current-evoked spikes at currents ≥150 pA ($P < 0.0001$, Figs. 5C and 5D). Resting membrane potential was not changed from control by MFQ in WT mice (Control 47.1 ± 2.3 mV, MFQ 47.2 ± 3.8 mV, $P = 0.1$). MFQ did not significantly reduce baseline firing rate in KO mice (Control 1.1 ± 0.3 Hz, MFQ 0.7 ± 0.2 Hz, $P = 0.2$, Figs. 5E and 5F), current-evoked spiking ($P > 0.2$, Figs. 5G and 5H), or RMP (Control 47.4 ± 2.1 mV, MFQ 52.1 ± 2.5 mV, $P = 0.17$). When comparing MFQ affects on the two strains of mice, there was no statistical difference between baseline and MFQ-treated DA neuron firing rate and current-evoked spiking in KO mice and MFQ-treated WT mice ($P > 0.5$ Fig. 5), and there was no difference in RMP between the two strains, with our without MFQ treatment ($P > 0.5$).

DISCUSSION

The aim of this study was to determine the role that Cx36 GJs play in regulating inhibitory synaptic activity in the VTA of juvenile mice. We were able to indentify VTA GABA neurons through the use of GAD67-GFP knock in mice, while DA neurons in GAD67-GFP knock-in and Cx36 KO mice were identified by previously-tested electrophysiological characteristics. The selective Cx36 GJ-blocker MFQ, and the less-selective GJ-blocker CBX, in conjunction with the use of Cx36 KO mice, were utilized to determine the role Cx36 GJs play in VTA inhibitory synaptic activity. The overall net physiologic effect the GJ blockers MFQ and CBX was to increase spike-dependent inhibition of VTA DA neurons, resulting in a decrease in VTA DA neuron firing rate and current-evoked spiking in WT, but not Cx36 KO, mice. Thus, blockade of GJs in WT mice, and the lack of GJs in Cx36 KO mice, may result in diminished DA neurotransmission in these mice. However, this study did not directly measure DA neurotransmission, therefore DA neurotransmission in KO mice may not be qualitatively or quantitatively comparable to that produced by the Cx36 blocker MFQ due to developmental adaptations. The fact that VTA DA neuron baseline firing rate was lower in Cx36 KO mice, and that both control and MFQ treated current-evoked spiking in KO mice was not significantly different from MFQ-treated WT mice strengthens the design concept of comparing these two mouse models to reveal GJ neurophysiology.

Mefloquine's marked increase in VTA DA sIPSCs in WT mice can be divided into two components: 1) An increase in nonspike-dependent GABA release, most-likely attributed to MFQ's ability to increase intracellular calcium; and 2) An increase in activity-dependent GABA release that we attribute to MFQ's selective blockade of Cx36 GJs. However, MFQ's increase in Cx36 KO mouse VTA DA sIPSCs only involved an increase in nonspike-dependent GABA release due to MFQ's calcium effect. These conclusions are supported by the fact that MFQ increased VTA DA neuron sIPSC frequency ~533% in WT mice, but only ~310% in Cx36 KO mice. Additionally, mIPSCs (a measure of nonactivity-dependent GABA release) were increased ~300% in both WT and Cx36 KO mice, but CBX, a less specific GJ blocker then MFQ, only increased sIPSC frequency in WT mice and did not affect mIPSCs in WT or KO mice. As seen by others, we also did note the baseline frequency of VTA DA neuron sIPSCs and mIPSCs in both WT and Cx36 mice were not statistically different, suggesting that much of the inhibition of VTA DA neurons is of a

tonic spontaneous nature. However, MFQ's ability to increase the frequency of sIPSCs and mIPSCs to different degrees demonstrates that we adequately dissected these two phenomena. This observation also points to the possibility that an effective mechanism for increasing inhibition of DA neurons would simply be reducing the electrical connectivity of GJ-connected VTA GABA neurons. We also noted that in the presence of CNQX and APV the baseline sIPSC and mIPSC baseline frequencies of WT and Cx36 KO mice where not significantly different. This lack of difference may be the result of adaptive compensatory mechanisms in the KO mouse. But as mentioned above, when comparing firing rate with no blockers present, the baseline firing rate of VTA DA neurons in Cx36 KO mice were significantly lower than WT mice (Fig. 5), but the same as WT mice treated with MFQ.

Of great interest was our discovery that MFQ did not increase VTA GABA neuron sIPSCs, suggesting that: (1) VTA GABA and DA neuron inhibitory synapses might not be physiologically homogeneous; (2) VTA GABA and DA neurons might be inhibited by at least two distinctly different subgroups of local-circuit GABA neurons: A subgroup with GJs that innervate VTA DA neurons; and a subgroup without GJs: or a GJ type other than Cx36 that innervate VTA GABA neurons (Hestrin and Galarreta, 2005). The differential effect of MFQ on DA and GABA neuron sIPSCs might also establish a possible mechanism for the negative side-effects of MFQ seen in humans stemming from the dysregulation of VTA DA neuron inhibition.

We are not alone in the observation that MFQ increases inhibition of midbrain DA neurons, or the idea that disruption of calcium regulation is involved. Zhou et al. (2006) found that in acutely dissociated brain slices, 3 μM MFQ induced a small increase in sIPSC frequency in midbrain DA neurons. However, at 25 μM we were unable to substantiate the claims by Zhou et al. that MFQ's increase in midbrain DA neuron sIPSC frequency was facilitated through cholinesterase inhibition, but we did provide additional support for the role calcium plays in this phenomenon. If not for carbenoxolone increasing spike-dependent IPSC frequency in WT mice similar to MFQ, and did not increase sIPSCs in Cx 36 mice, most of MFQ's effects could be attributed to a potent nonspecific calcium effect. A possible explanation for the difference in concentrations of MFQ needed to increase VTA DA neuron sIPSC frequency in these studies may be that the effective concentration of MFQ is lower in brain slice tissue as opposed to the acutely dissociated slices used by Zhou, perhaps as a result of the difficulty of MFQ to penetrate into brain slices (Cruikshank et al., 2004). The difficulty of MFQ's ability to penetrate brain slice tissue is made more difficult by its propensity to bind tightly to phospholipid membranes. We also tested the effects of odansetron as a control against MFQ's reported $5HT_3$ receptor antagonism, to eliminate the possibility that the increase in DA neuron sIPSC frequency could be attributed to this MFQ effect. MFQ's effects on sIPSCs were not mimicked by odansetron, rather odansetron suppressed sIPSC frequency, presenting another possible nonspecific drug effect of MFQ that could contribute to its side effects reported in humans.

Electrical synapses (composed of Cx36 GJs) connecting inhibitory interneurons are common in certain areas of the brain (for review Connors and Long, 2004), including the midbrain, and participate in the intercellular spread of ions, small molecules, and the propagation of oscillatory patterns (Landisman and Connors, 2005) and spike synchrony (Galarreta and

Hestrin, 2001; Szabadics et al., 2001). We have previously shown that VTA GABA neurons evince ultra-structural evidence for GJs (Steffensen et al., 1998), express Cx36 mRNA and protein (Allison et al., 2006), dye couple (Allison et al., 2006), spike couple (Stobbs et al., 2004), discharge multiply with afferent stimulation (Lassen et al., 2007), which is blocked by MFQ, and appear to form part of a larger syncytium of GABA neurons in the reticular formation (Lassen et al., 2007). This study was performed on juvenile mice, and while the role of GJs in the intact adult brain is not known, the mechanistic focus has traditionally been on the open GJ in the context of spike synchrony and shared excitability. A paper from our lab describing differences in DA and GABA neurons between adult WT and KO adult mice is currently in press. This study presents the view of GJs as being more akin to variable resistors that effect cellular and network physiology in both open and closed conformations. With this view of GJ physiology, a possible explanation for the data presented here is that when MFQ blocks GJs the electrically-coupled VTA GABA network becomes uncoupled, releasing each cell from the resistive network load. The result being that individual GABA neuron activity is no longer synchronized with its neighboring GABA neurons, but rather is released from the resistive load of the network and thus enabled to fire more autonomously. But whether GJ-mediated interneuron synchrony facilitates faster firing, slower firing, or both depending on where the GJs are located and whether their currents are timed with transmitter release (Buzsaki and Chrobak, 1995; Szabadics et al., 2001; Tamas et al., 2000), it appears from this study that blocking Cx36 GJs leads to greater release of GABA onto target neurons, in this case DA neurons in juvenile mice. The findings of this study strengthen the argument that GJs serve as critical modulators of brain activity and may serve as strategic targets for the clinical treatment of many disorders involving the mesolimbic DA system.

Acknowledgments

Contract grant sponsor: PHS; Contract grant number: AA13666.

REFERENCES

Allison DW, Ohran AJ, Stobbs SH, Mameli M, Valenzuela CF, Sudweeks SN, Ray AP, Henriksen SH, Steffensen SC. Connexin-36 gap junctions mediate electrical coupling between ventral tegmental area GABA neurons. Synapse. 2006; 60:20–31. [PubMed: 16575850]

Buzsaki G, Chrobak JJ. Temporal structure in spatially organized neuronal ensembles: A role for interneuronal networks. Curr Opin Neurobiol. 1995; 5:504–510. [PubMed: 7488853]

Caridha D, Yourick D, Cabezas M, Wolf L, Hudson TH, Dow GS. Mefloquine-induced disruption of calcium homeostasis in mammalian cells is similar to that induced by ionomycin. Antimicrob Agents Chemother. 2008; 52:684–693. [PubMed: 17999964]

Carr DB, Sesack SR. GABA-containing neurons in the rat ventral tegmental area project to the prefrontal cortex. Synapse. 2000a; 38:114–123. [PubMed: 11018785]

Carr DB, Sesack SR. Projections from the rat prefrontal cortex to the ventral tegmental area: Target specificity in the synaptic associations with mesoaccumbens and mesocortical neurons. J Neurosci. 2000b; 20:3864–3873. [PubMed: 10804226]

Connors BW, Long MA. Electrical synapses in the mammalian brain. Annu Rev Neurosci. 2004; 27:393–418. [PubMed: 15217338]

Cruikshank SJ, Hopperstad M, Younger M, Connors BW, Spray DC, Srinivas M. Potent block of C×36 and C×50 gap junction channels by mefloquine. Proc Natl Acad Sci USA. 2004; 101:12364–12369. [PubMed: 15297615]

Deans MR, Gibson JR, Sellitto C, Connors BW, Paul DL. Synchronous activity of inhibitory networks in neocortex requires electrical synapses containing connexin36. Neuron. 2001; 31:477–485. [PubMed: 11516403]

Dow GS, Hudson TH, Vahey M, Koenig ML. The acute neurotoxicity of mefloquine may be mediated through a disruption of calcium homeostasis and ER function in vitro. Malar J. 2003; 2:14. [PubMed: 12848898]

Dow GS, Koenig ML, Wolf L, Gerena L, Lopez-Sanchez M, Hudson TH, Bhattacharjee AK. The antimalarial potential of 4-quinolinecarbinolamines may be limited due to neurotoxicity and cross-resistance in mefloquine-resistant Plasmodium falciparum strains. Antimicrob Agents Chemother. 2004; 48:2624–2632. [PubMed: 15215119]

Fields HL, Hjelmstad GO, Margolis EB, Nicola SM. Ventral tegmental area neurons in learned appetitive behavior and positive reinforcement. Annu Rev Neurosci. 2007; 30:289–316. [PubMed: 17376009]

Galarreta M, Hestrin S. Spike transmission and synchrony detection in networks of GABAergic interneurons. Science. 2001; 292:2295–2299. [PubMed: 11423653]

Hestrin S, Galarreta M. Electrical synapses define networks of neocortical GABAergic neurons. Trends Neurosci. 2005; 28:304–309. [PubMed: 15927686]

Ikemoto S. Dopamine reward circuitry: Two projection systems from the ventral midbrain to the nucleus accumbens-olfactory tubercle complex. Brain Res Rev. 2007; 56:27–78. [PubMed: 17574681]

Johnson SW, North RA. Two types of neurone in the rat ventral tegmental area and their synaptic inputs. J Physiol (Lond). 1992; 450:455–468. [PubMed: 1331427]

Juszczak GR, Swiergiel AH. Properties of gap junction blockers and their behavioural, cognitive and electrophysiological effects: Animal and human studies. Prog Neuropsychopharmacol Biol Psychiatry. 2009; 33:181–198. [PubMed: 19162118]

Landisman CE, Connors BW. Long-term modulation of electrical synapses in the mammalian thalamus. Science. 2005; 310:1809–1813. [PubMed: 16357260]

Lassen MB, Brown JE, Stobbs SH, Gunderson SH, Maes L, Valenzuela CF, Ray AP, Henriksen SJ, Steffensen SC. Brain stimulation reward is integrated by a network of electrically coupled GABA neurons. Brain Res. 2007; 1156:46–58. [PubMed: 17524371]

Margolis EB, Lock H, Hjelmstad GO, Fields HL. The ventral tegmental area revisited: Is there an electrophysiological marker for dopaminergic neurons? J Physiol. 2006; 577(Part 3):907–924. [PubMed: 16959856]

Margolis EB, Mitchell JM, Ishikawa J, Hjelmstad GO, Fields HL. Midbrain dopamine neurons: Projection target determines action potential duration and dopamine D(2) receptor inhibition. J Neurosci. 2008; 28:8908–8913. [PubMed: 18768684]

McArdle JJ, Sellin LC, Coakley KM, Potian JG, Hognason K. Mefloquine selectively increases asynchronous acetylcholine release from motor nerve terminals. Neuropharmacology. 2006; 50:345–353. [PubMed: 16288931]

Omelchenko N, Sesack SR. Laterodorsal tegmental projections to identified cell populations in the rat ventral tegmental area. J Comp Neurol. 2005; 483:217–235. [PubMed: 15678476]

Omelchenko N, Sesack SR. Cholinergic axons in the rat ventral tegmental area synapse preferentially onto mesoaccumbens dopamine neurons. J Comp Neurol. 2006; 494:863–875. [PubMed: 16385486]

Schlagenhauf P, Johnson R, Schwartz E, Nothdurft HD, Steffen R. Evaluation of mood profiles during malaria chemoprophylaxis: A randomized, double-blind, four-arm study. J Travel Med. 2009; 16:42–45. [PubMed: 19192127]

Steffensen SC, Svingos AL, Pickel VM, Henriksen SJ. Electro-physiological characterization of GABAergic neurons in the ventral tegmental area. J Neurosci. 1998; 18:8003–8015. [PubMed: 9742167]

Steffensen SC, Taylor SR, Horton ML, Barber EN, Lyle LT, Stobbs SH, Allison DW. Cocaine disinhibits dopamine neurons in the ventral tegmental area via use-dependent blockade of GABA neuron voltage-sensitive sodium channels. Eur J Neurosci. 2008; 28:2028–2040. [PubMed: 19046384]

Stobbs SH, Ohran AJ, Lassen MB, Allison DW, Brown JE, Steffensen SC. Ethanol suppression of ventral tegmental area GABA neuron electrical transmission involves NMDA receptors. J Pharmacol Exp Ther. 2004; 311:282–289. [PubMed: 15169831]

Szabadics J, Lorincz A, Tamas G. Beta and gamma frequency synchronization by dendritic gabaergic synapses and gap junctions in a network of cortical interneurons. J Neurosci. 2001; 21:5824–5831. [PubMed: 11466454]

Tamamaki N, Yanagawa Y, Tomioka R, Miyazaki J, Obata K, Kaneko T. Green fluorescent protein expression and colocalization with calretinin, parvalbumin, and somatostatin in the GAD67-GFP knock-in mouse. J Comp Neurol. 2003; 467:60–79. [PubMed: 14574680]

Tamas G, Buhl EH, Lorincz A, Somogyi P. Proximally targeted GABAergic synapses and gap junctions synchronize cortical interneurons. Nat Neurosci. 2000; 3:366–371. [PubMed: 10725926]

Thompson AJ, Lummis SC. Antimalarial drugs inhibit human 5-HT(3) and GABA(A) but not GABA(C) receptors. Br J Pharmacol. 2008; 153:1686–1696. [PubMed: 18311193]

Tran TM, Browning J, Dell ML. Psychosis with paranoid delusions after a therapeutic dose of mefloquine: A case report. Malar J. 2006; 5:74. [PubMed: 16925829]

Wise RA. Dopamine, learning and motivation. Nat Rev Neurosci. 2004; 5:483–494. [PubMed: 15152198]

Wooltorton E. Mefloquine: Contraindicated in patients with mood, psychotic or seizure disorders. CMAJ. 2002; 167:1147. [PubMed: 12427708]

Zhou C, Xiao C, McArdle JJ, Ye JH. Mefloquine enhances nigral gamma-aminobutyric acid release via inhibition of cholinesterase. J Pharmacol Exp Ther. 2006; 317:1155–1160. [PubMed: 16501066]

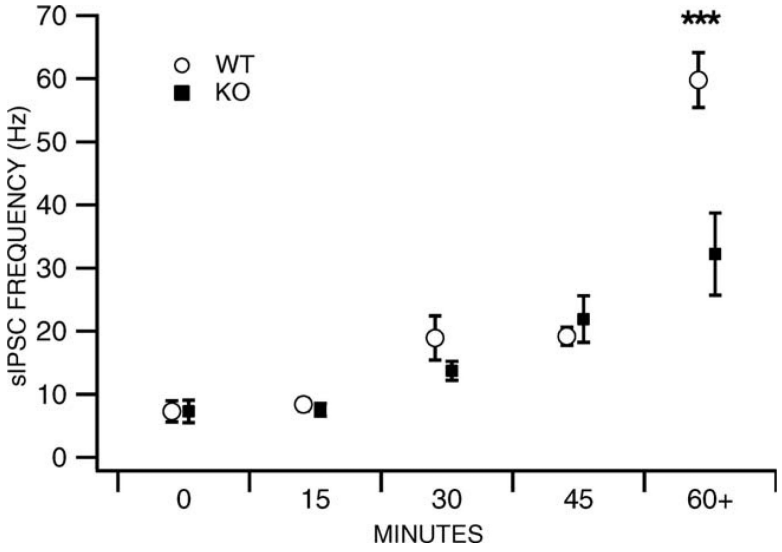

Fig. 1.

Time course of mefloquine effects on VTA dopamine neuron sIPSC frequency. VTA DA neuron sIPSCs were recorded at 15-min intervals in wildtype (WT, open circle) and Cx36 KO (filled squares) mice with bath-applied MFQ (25 μM), D-APV (50 μM), and CNQX (30 μM). MFQ increased sIPSC frequency similar in both WT and Cx36 KO mice until the 60+ min time point when WT sIPSCs were 175% of KO mice sIPSCs, $P = 0.0001$. WT data: 7.3 ± 1.7 Hz ($t = 0$); 8.4 ± 0.9 Hz (15 min); 18.9 ± 3.5 Hz (30 min); 19.2 ± 1.4 Hz (45 min); 59.8 ± 4.3 Hz (60 min). Cx36 KO data: 7.3 ± 1.0 Hz ($t = 0$) to: 7.5 ± 0.9 Hz (15 min); 13.7 ± 1.6 Hz (30 min); 21.9 ± 3.7 Hz (45 min); 32.2 ± 6.5 Hz (60 min).

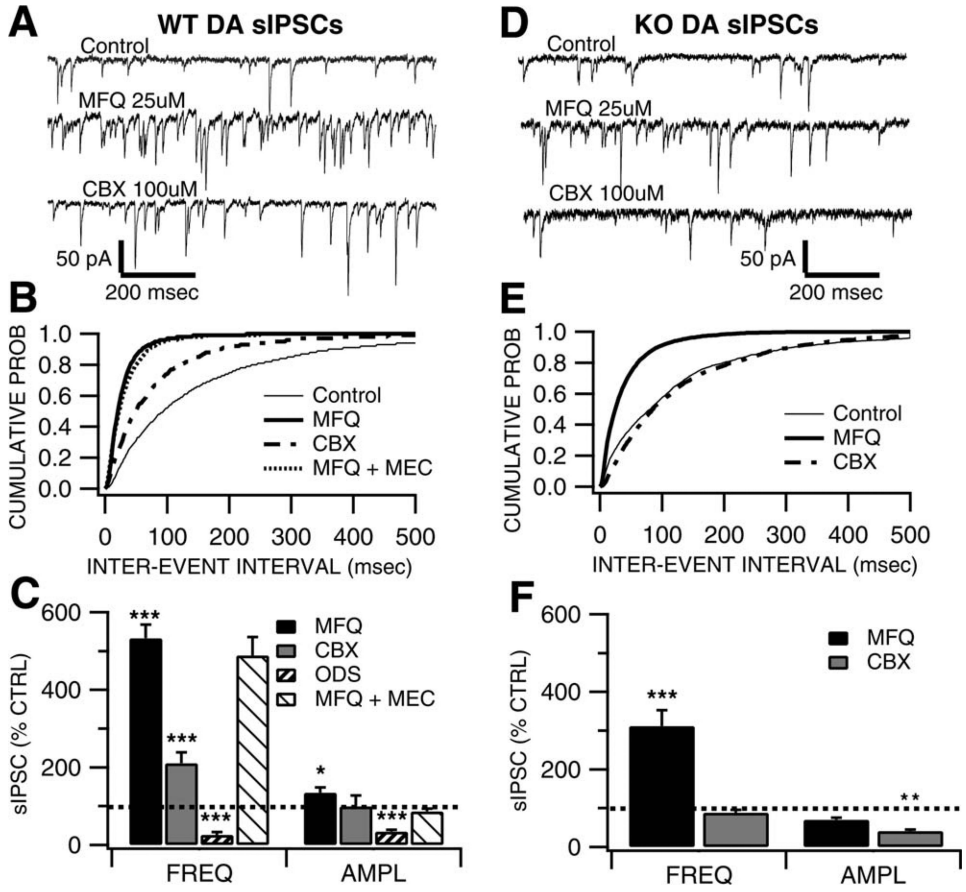

Fig. 2.

Mefloquine effects on VTA dopamine neuron sIPSC frequency, amplitude, and interevent interval in WT and Cx36 KO mice. This figure compares WT (**A–C**) and KO (**D–F**) VTA DA neuron sIPSC data after being presoaked with either MFQ (25 μM), CBX (100 μM), ODS (25 μM), or MFQ (25 μM) 1 MEC (10 μM) for ≥60 min. In WT mice (C), sIPSCs were increased similarly by MFQ (533%) and MFQ+MEC (488%), CBX alone increased sIPSC frequency 211%, but ODS alone did not mimic MFQ. MFQ and MFQ+MEC shifted the interevent interval curve to the left (B), while CBX alone shifted the curve slightly to the left. In Cx36 KO mice, only MFQ increased sIPSC frequency (F) and shifted the interevent interval curve to the left (E). MFQ's increase of Cx36 KO mouse sIPSC frequency was about half of its increase of WT sIPSC frequency.

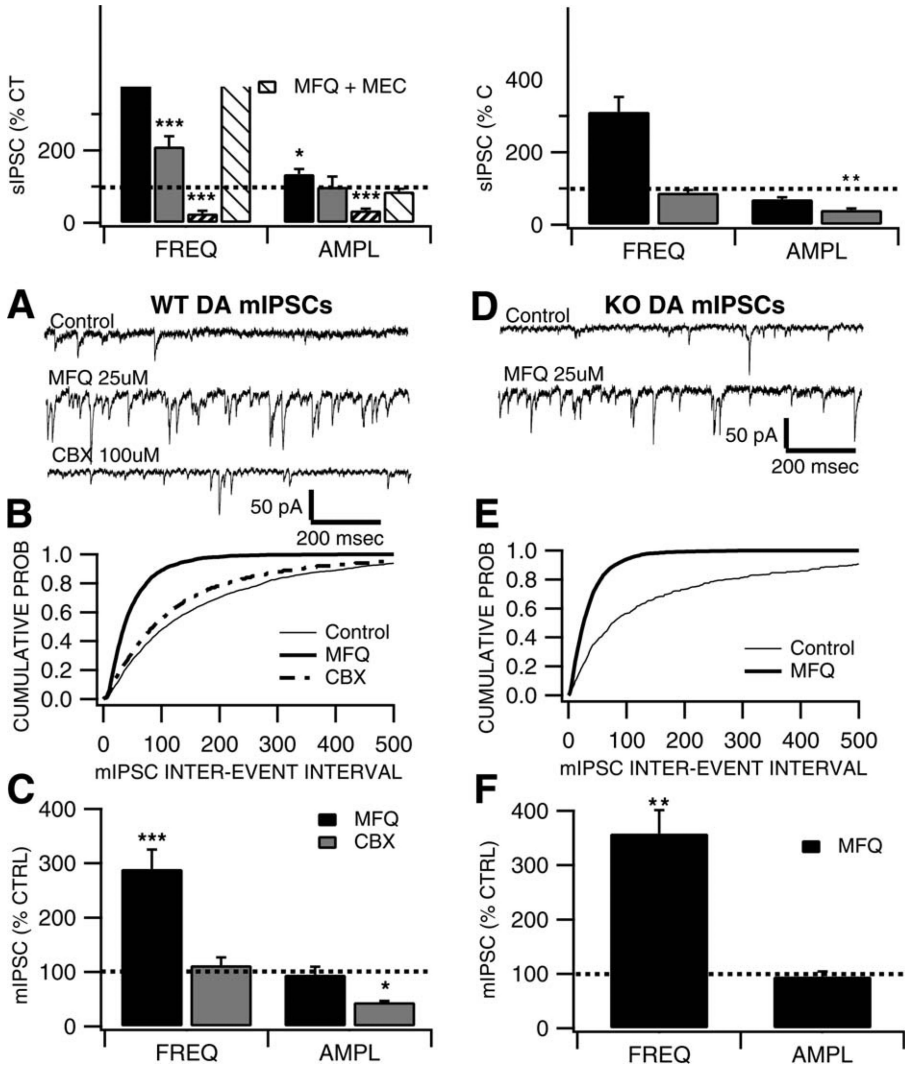

Fig. 3.

Mefloquine effects on VTA dopamine neuron mIPSC frequency, amplitude, and interevent interval in WT and Cx36 KO mice: This figure compares WT (**A–C**) and KO (**D–F**) VTA DA neuron mIPSC data after being presoaked with MFQ (25 μM) or CBX (100 μM) for ≥60 min. In WT mice (C), mIPSCs were increased (289%) by MFQ but not at all by CBX (100 μM). In WT mice, MFQ but not CBX shifted the interevent interval curve to the left (B). In Cx36 KO mice, MFQ (25 μM) increased mIPSC frequency 358% (F) and shifted the interevent interval plot to the left (E).

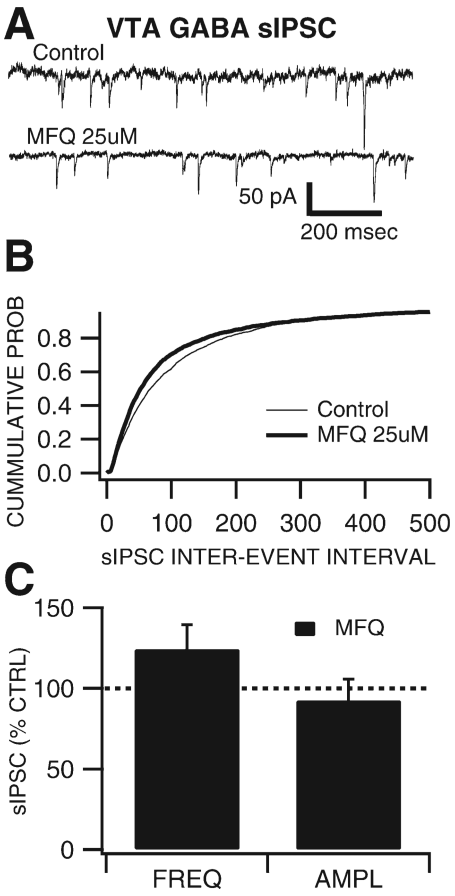

Fig. 4.

Mefloquine does not affect VTA GABA neuron sIPSC frequency. This figure diagrams presoaked MFQ (25 μM) effects on WT VTA GABA neuron sIPSCs. MFQ did not increase VTA GABA neurons sIPSC frequency (**A, C**) or shift the interevent distribution plot (**B**).

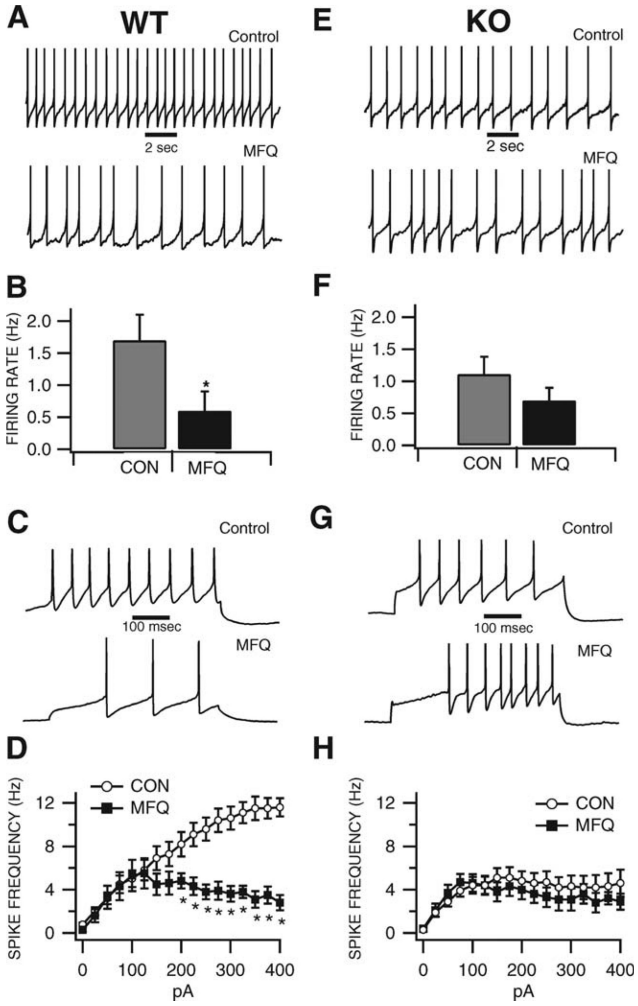

Fig. 5.

MFQ reduces VTA DA neuron firing rate and current-evoked spiking. This figure compares WT (**A–D**) and KO (**E–H**) VTA DA neuron spontaneous firing rate and current-evoked spikes after being presoaked with MFQ (25 μM). (A, E) Raw traces of WT and KO mouse VTA DA neuron spontaneous firing rate voltage spikes. (B, F) These panels show the summary of all spontaneous firing rate experiments in WT and KO mice in which MFQ significantly decreased firing rate in WT mice but not it Cx36 KO mice. Note that Cx36 KO mouse baseline firing rate is lower than WT mouse baseline firing rate. Panels C and G show raw traces of current-evoked spiking in WT and KO mice in which MFQ reduced current-evoked spiking at all currents greater than 125pA (D), but had no effect on already reduced Cx36 KO mouse spiking (H). Note that Cx36 KO mouse control and MFQ-treated current-evoked spiking are similar to WT MFQ-treated current-evoked spiking.